CHEMISTRY
A EUROPEAN JOURNAL

DOI: 10.1002/chem.201100458

Homogeneous Nucleophilic Radiofluorination and Fluorination with Phosphazene Hydrofluorides

Bente Mathiessen, Andreas T. I. Jensen, and Fedor Zhuravlev*[a]

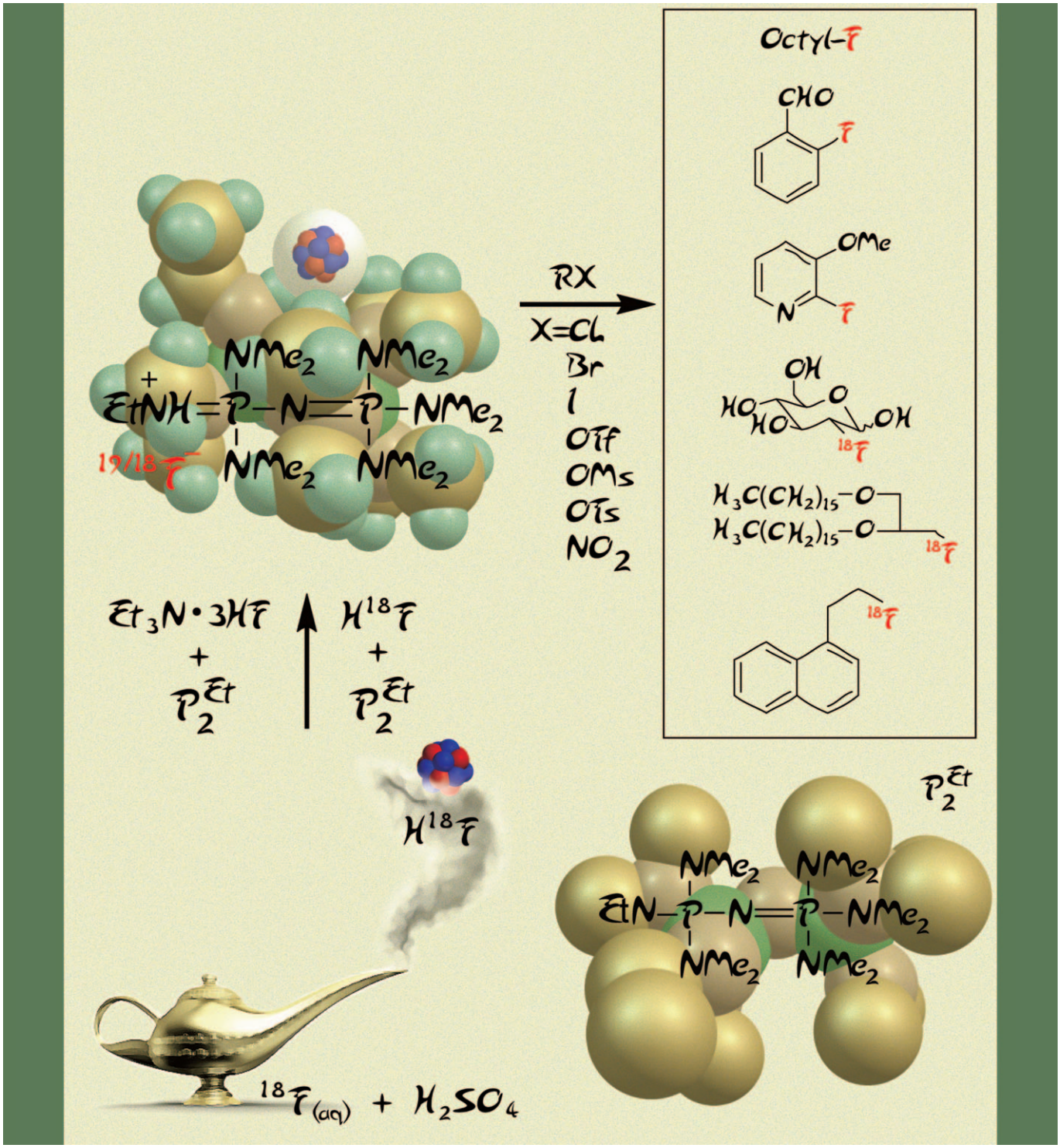

Abstract: A series of phosphazenium hydrofluorides, P_1^{tBu}·[$^{18/19}$F]HF, P_1^{tOct}·[$^{18/19}$F]HF, P_2^{Et}·[$^{18/19}$F]HF, and P_4^{tBu}·[$^{18/19}$F]HF, was synthesized. The radioactive phosphazenium [^{18}F]hydrofluorides were obtained by the one-step formation and trapping of gaseous [^{18}F]HF with the respective phosphazene bases. The [^{19}F] isotopomers were prepared from the corresponding phosphazene bases and Et_3N·3HF. Under the design of experiment (DoE)-optimized conditions, P_2^{Et}·HF and P_4^{tBu}·HF fluorinated alkyl chlorides, bromides, and pseudohalides in 76–98% yield, but gave lower yields with iodides and electron-deficient arenes. DoE models showed that fluorination can be performed in glass vessels, and that the reactivity of P_2^{Et}·HF and P_4^{tBu}·HF is dominated by solvent polarity but is insensitive to water to at least 2 equiv. In contrast, P_1^{tBu}·HF and P_1^{tOct}·HF were unstable towards autofluorolysis. DFT calculations were performed to rationalize this finding in terms of diminished steric bulk, higher Parr's electrophilicity, and chemical hardness of $P_1^{R}H^+$. The corresponding radiofluorination reaction gave no valid DoE model but displayed similar substrate scope. High specific activity and excellent radiochemical yields with various pseudohalides (81–91%) suggest that the proposed radiofluorination methodology can complement the current [^{18}F]KF/Kryptofix methods, particularly in the areas for which nonpolar reaction conditions are required.

Keywords: fluorides · fluorination · nucleophilic substitution · phosphazenes · radiochemistry

Introduction

Over the years positron emission tomography (PET) has become an essential research and medical imaging modality.[1] Among different radioisotopes, biopharmaceutically[2] and PET friendly[3] [^{18}F]fluorine is currently the most widely used. This drives the production of vintage[4] and the development of novel radiolabeled compounds.[5] As the 21st century technology of medical isotope production is gearing toward process automation[6] and device miniaturization,[7] one can anticipate that much of the future technical development will be shaped by the Procrustean bed of [^{18}F]fluoride recovery and processing. In practice, if one wants to obtain [^{18}F]fluorine in its highest specific activity one needs to run an $^{18}O(p,n)^{18}F$ reaction: the cyclotron-accelerated proton bombardment of [^{18}O]-enriched H_2O, which yields [^{18}F]fluoride as a water solution. At -104 kcal mol^{-1} of estimated free energy of hydration,[8] [^{18}F]fluoride in water is nucleophilically inert. To restore its intrinsic nucleophilicity, water must be removed. In routine production, this is typically achieved by trapping [^{18}F]fluoride on an ion-exchange column and subsequent elution with a kryptand, followed by repeated azeotropic evaporation of water. Due to the relatively short half-life of the radioisotope ($t_{1/2} = 110$ min) and apparatus miniaturization requirements, simpler and more expeditious processes are sought after. The water evaporation step is often targeted for optimization,[9] and in some cases can be skipped altogether, for example: 1) by using ionic liquids;[10] 2) by eluting [^{18}F]fluoride with strong organic base and protic additives;[11] 3) with polymer, loaded with alkylammonium carbonate;[12] 4) by radiofluorination performed directly on the resin;[13] and 5) by using a polydimethylsiloxane matrix for solvent exchange inside a microreactor.[7]

Our approach to [^{18}F]fluoride recovery and radiofluorination was guided by the following considerations: 1) the recovery of [^{18}F]fluoride and its intrinsic nucleophilicity must be achieved in no more than one step, physical or chemical; 2) to accommodate a wide range of biologically interesting substrates, including lipophilic, [^{18}F]fluoride must be soluble in both polar and nonpolar solvents; and 3) the radiochemical yield must be at least 50% relative to target water. We became interested in alternative methods for a single-step [^{18}F]fluoride recovery and nucleophilic activation. It occurred to us that instead of removing water from the radionuclide one can distill it as hydrogen fluoride gas.[14] This approach also has a corollary advantage as a chemical and radiochemical purification. Once liberated, [^{18}F]HF can be trapped as *N*-onium hydrofluoride by using a strong organic base. Fluorination with organic base–hydrogen fluoride adducts, such as Olah's reagent (pyridine·*n*HF),[15] Franz reagent (Et_3N·3HF),[16] and ether-based HF adducts[17] is well precedented. Although readily available and moderately reactive, they have an unfortunate tendency to dissociate HF, thereby etching glass and causing side reactions. HF adducts of stronger bases, such as proton sponge, are less prone to dissociation, which allows for fluorination[18] and radiofluorination[19] of activated heterocycles. We hypothesized that stronger organic bases, such as Schwesinger's phosphazenes,[20b] would effectively suppress HF dissociation. Additionally, we believed that their bulk and globular shape would create a cation/anion mismatch, thus resulting in increased solubility and fluoride nucleophilicity. In tandem with radiofluorination we also investigated nonradioactive fluorination. This served two purposes: 1) fluorination would act as an isotopic "Sherpa" providing us with trackable or isolable products or intermediates and assisting in understanding the underlying chemistry; and 2) we also expected that this study would

[a] B. Mathiessen, A. T. I. Jensen, Dr. F. Zhuravlev
Hevesy Laboratory, Technical University of Denmark
Risø National Laboratory for Sustainable Energy
Frederiksborgvej 399, P.O. Box 49, 4000 Roskilde (Denmark)
Fax: (+45) 46775347
E-mail: fezh@risoe.dtu.dk

Supporting information for this article is available on the WWW under http://dx.doi.org/10.1002/chem.201100458.

result in the development of a synthetically useful homogeneous fluorination methodology, applicable to a wide range of conditions and substrates.

Results and Discussion

Synthesis and characterization of P_n^R·HF: P_1^{tBu}·HF, P_1^{tOct}·HF, P_2^{Et}·HF, and P_4^{tBu}·HF were prepared by adding $^1/_3$ equiv of Et_3N·3HF to the solution of the corresponding phosphazene bases (Scheme 1) in diethyl ether [Eq. (1)]:

$$P_n^R + Et_3N \cdot 3HF \rightarrow P_n^R \cdot HF + Et_3N \cdot 2HF$$

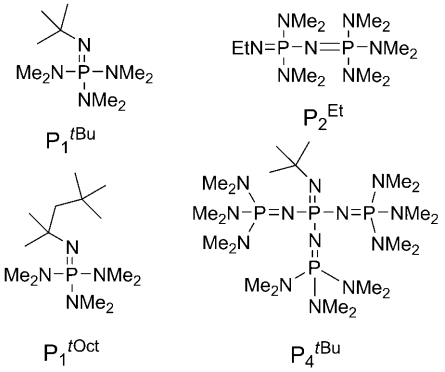

Scheme 1. Schwesinger's phosphazene bases P_n^R used in this study.

P_1^{tBu}·HF, P_1^{tOct}·HF, and P_4^{tBu}·HF precipitated out as very hygroscopic white solids; P_2^{Et}·HF separated as a mildly hygroscopic viscous oil. The compounds displayed prominent P_n^R·H^+ peaks in the positive mode of ESI-MS, and share many ^{1}H, ^{13}C, and ^{31}P NMR features with the reported earlier peralkyl phosphazenium cations. [20a] The ^{19}F chemical shifts for fluoride were found in the range of −150 to −153 ppm, which was consistent with the chemical shifts reported for other quaternary *N*-onium fluorides.[21] The synthesized P_n^R·HF were soluble in polar organic solvents, and also in benzene and toluene.

Synthesis of P_n^R·[^{18}F]HF: We envisioned that the P_n^R·[^{18}F]HF series of compounds could be obtained by reacting [^{18}F]HF with the corresponding phosphazene bases [Eq. (2)]:

$$P_n^R + [^{18}F]HF \rightarrow P_n^R \cdot [^{18}F]HF$$

[^{18}F]HF was generated by adding [^{18}O]-enriched cyclotron-irradiated water to 98% sulfuric acid. The flow of Ar carried the liberated hydrogen fluoride to a trap containing a solution of P_n^R base in toluene. At the outset, we recognized that the large hydration energy of hydrogen fluoride,[22] its room-temperature boiling point (19.5 °C), and the high viscosity of its H_2SO_4 solution would significantly affect the liberation efficiency of gaseous [^{18}F]HF. Another concern was the adsorption of [^{18}F]HF to the reaction vessel and the tubing of the apparatus. The initial runs in polyethylene (PE) vials at room temperature yielded only traces of [^{18}F]fluorine activity in the trap. Running the reaction at 85 °C while vigorously (300 ccm min^{-1}) purging the solution with Ar improved radioactivity transfer to 39% (average of 22 runs). As a means to degas the bulk of the liquid and to reduce the adsorption of [^{18}F]HF to the surface, we ran the [^{18}F]HF synthesis in a glassy carbon vessel while applying constant ultrasound irradiation (240 W/35 kHz, 30 min). This proved successful: radioactivity transfer as high as 82% with an average of 71% could be achieved. Our attempts to characterize the synthesized P_n^R·[^{18}F]HF by comparing their retention times with those of the stable isotope analogues using radio-TLC or radio-HPLC were stymied by extensive line broadening and decomposition on the sorbent.

Initial P_n^R hydrofluoride screening: With P_n^R hydrofluorides in hand we turned to screening studies. Our objective was to identify a set of reaction conditions that had a statistically significant influence on the outcome of the fluorination. To simplify the screening we adopted a stepwise strategy. First, we ran both fluorination and radiofluorination with a set of P_n^R hydrofluorides under the same, albeit arbitrary, reaction conditions. The most active P_n^R hydrofluoride was then submitted to a series of experiments, in which we simultaneously varied a number of reaction parameters. The fluorination was performed in toluene at 100–120 °C with 1-chlorooctane as substrate. 1-Naphthalenethyl methanesulfonate,[23] a substrate containing a UV chromophore, was chosen for radiofluorination under similar reaction conditions. The results of the P_n^R hydrofluoride screening are shown in Table 1.

A control experiment showed that the reference Et_3N·3HF and Et_3N·[^{18}F]HF were inactive under the reaction conditions. Surprisingly, the P_1^R hydrofluorides also failed to give more than a trace level of products (Table 1, entries 3–6). On the other hand, P_2^{Et} and P_4^{tBu} hydrofluorides showed promising results in both fluorination (Table 1, entries 7 and 9) and radiofluorination (Table 1, entries 8 and 10). P_2^{Et} hydrofluoride, cheaper and less hygroscopic than its P_4^{tBu} congener, was chosen to enter the second stage of the screening process, in which we examined the influence of solvent, water content, and reaction vessel material.

Fluorination: screening the reaction conditions: The choice of reaction factors was guided by the following considerations. Fluoride is a powerful base[24] with enormous hydration energy.[8] Solvent polarity and hydration level are known to strongly affect fluoride's nucleophilicity and basicity.[25] The latter has another important ramification. In the majority of reported onium hydrofluorides, the fluoride anion successfully competes with the organic base for the proton, forming HF. Partial dissociation of HF, which leads to polyhydrofluorides, has been documented for pyridine,[15] triethylamine,[16b] and proton sponge hydrofluorides.[26] The dissociated HF is known to attack borosilicate glass.[16b] In our case, glass etching by [^{18}F]HF would have a particularly

Table 1. Initial screening of P_n^R hydrofluorides for fluorination and radiofluorination efficiency.[a]

Entry	Reagent	Substrate	Yield [%][b]
1	$Et_3N{\cdot}3HF$	octyl-Cl	NR[c]
2	$Et_3N{\cdot}[^{18}F]HF$	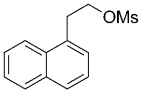	NR
3	$P_1^{tBu}{\cdot}HF$	octyl-Cl	traces
4	$P_1^{tOct}{\cdot}HF$	octyl-Cl	traces
5	$P_1^{tBu}{\cdot}[^{18}F]HF$	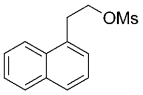	0.6
6	$P_1^{tOct}{\cdot}[^{18}F]HF$	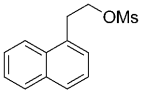	0.4
7	$P_2^{Et}{\cdot}HF$	octyl-Cl	29
8	$P_2^{Et}{\cdot}[^{18}F]HF$	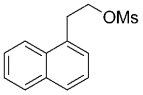	85
9	$P_4^{tBu}{\cdot}HF$	octyl-Cl	38
10	$P_4^{tBu}{\cdot}[^{18}F]HF$	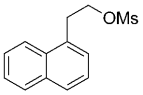	70

[a] Fluorination: 1-chlorooctane, $P_n^R{\cdot}HF$ (0.18 M), toluene, 100 °C, 1 h; radiofluorination: 1-naphthalenethyl methanesulfonate (52 μmol), 120 °C, 20 min. [b] Chemical or radiochemical yields as determined by GC or radio-TLC after purification on silica Sep-Pak. [c] NR: no reaction.

detrimental effect as it would lead to trapping of $[^{18}F]$fluoride in the walls of the reaction vessel. It was therefore important to consider the effect of the reaction vessel material. Because the underlying reason for the above-mentioned effects is ultimately rooted in the strength of the H–F bond, it was conceivable that the experimental factors we have just discussed are correlated. Therefore, a screening methodology that relies on the traditional "changing one separate factor at a time" (COST) approach would be a poor strategy, as it would fail to unravel a correlation if it existed. An unreasonably large number of experiments and the propensity to fall into local minima are other disadvantages of the COST method. A better approach was to use a multivariate statistical experimental design known as the design of experiment (DoE).[27] In DoE, the factors deemed important are systematically and simultaneously varied, thus allowing for statistically driven analysis of correlated data in a limited number of experiments. Changing the experimental conditions (factors) according to the DoE algorithm, and consequently measuring the results of the experiments (responses) would produce a model, typically in the polynomial form. The sign and the relative value of the coefficients define the contribution of the factor to the overall model. Table 2 describes our experimental design.

A reaction matrix, consisting of eight experiments plus three central point replicates (Table 2, entries 9–11) was generated by using a specialized DoE software

Table 2. Screening the reaction conditions: two-level full factorial design and results for fluorination of 1-chlorooctane with $P_2^{Et}{\cdot}HF$[a].

Entry	Solvent	Reaction vessel	H_2O equiv.	Conversion [%][b]	1-Fluorooctane yield [%][b]	1-Octene yield [%][b]
1	toluene	steel	0	41	17	2
2	HMPA	steel	0	55	28	13
3	toluene	glass	0	40	28	3
4	HMPA	glass	0	67	17	10
5	toluene	steel	2	11	6	0
6	HMPA	steel	2	57	34	9
7	toluene	glass	2	34	29	3
8	HMPA	glass	2	69	29	10
9	toluene	steel	1	25	23	3
10	toluene	steel	1	17	18	2
11	toluene	steel	1	28	14	1

[a] Reaction conditions: 1-chlorooctane, $P_2^{Et}{\cdot}HF$ (0.18 M), 100 °C, 2 h. [b] Determined by GC.

MODDE 9.0.[28] Three reaction factors were varied: the solvent polarity, the amount of water, and the reaction vessel material. We chose toluene as a nonpolar solvent ($E_T^N = 0.099$) and hexamethylphosphoramide (HMPA; $E_T^N = 0.315$)[29] as a polar aprotic solvent. The level of hydration was controlled by adding water to the reaction mixture. For each experiment we recorded three responses: the yield of the desired S_N2 product (1-fluorooctane), the yield of E2 byproduct (1-octene), and the conversion of the starting material. Fitting the data with partial least-squares (PLS) regression (MODDE) resulted in a statistically satisfactory model for all three responses (see the Supporting Information). The examination of the model coefficients revealed a number of interesting features. As expected, HMPA increased the reactivity of the substrate and promoted E2 elimination (Figure 1, red bars). The reaction vessel material was important: the conversion of the substrate was faster in a glass reaction vessel, but slower in a steel container (Figure 1, blue bars). There was also a small but statistically significant contribution to the yield from a correlated effect of reaction vessel material and the solvent. A combination of toluene in glass or HMPA in steel increased the yield, whereas the opposite combination decreased it (Figure 1, cyan bars). Surprisingly, water did not have any statistically significant effect on either the conversion or the yield (the confidence intervals for the corresponding coefficients cross the zero line).

Fluorination: optimizing the reaction conditions: The model resulting from the screening experiments identified the important factors to be used later in optimization studies. To minimize byproduct formation we optimized fluorination with respect to both the fluoride yield and substrate selectivity. The solvent polarity was chosen as a quantitative parameter for optimization as it affected the rates of both conversion and elimination. From a practical point of view, we also felt it was necessary to substitute toxic HMPA for a benign polar aprotic solvent. Unfortunately, the attempt to use DMSO led to oxidation of the substrate to 1-octanal in what

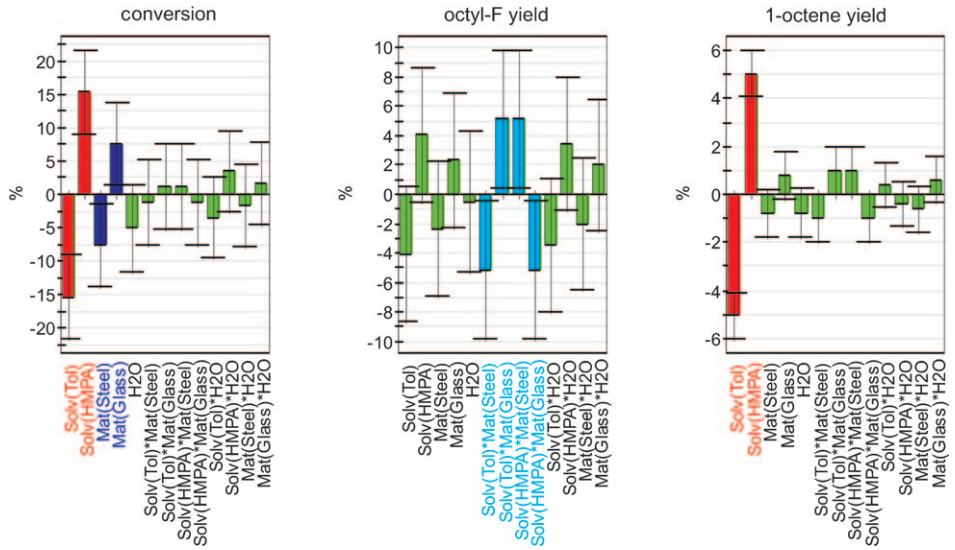

Figure 1. Regression coefficients for the screening model: the effect of reaction parameters (x axis) on 1-chlorooctane conversion (left), 1-fluorooctane yield (center), and 1-octene yield (right). Tol: toluene.

appears to be a Swern-like process,[30] driven by the basicity of fluoride (Scheme 2).

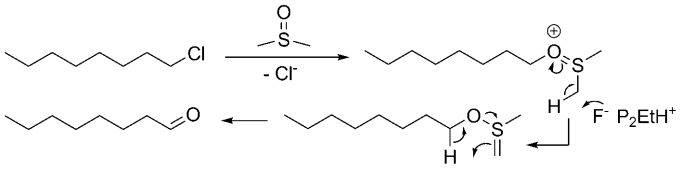

Scheme 2. Oxidation of 1-chlorooctane with DMSO in the presence of P_2^{Et}HF.

DMF and tetramethylurea (tmeu) were found to be good alternatives to HMPA. Tmeu was subsequently chosen as solvent because its hexane miscibility was compatible with our GC protocol. Reaction temperature was chosen as another quantitative factor. Due to a wider range of reaction temperatures required for optimization runs, we used high-boiling mesitylene (Mes) instead of toluene. Because glass was well tolerated and the chemistry was insensitive to moisture, we ran the optimization in glass reaction vessels in HPLC-grade solvents. Once again, 1-chlorooctane was used as a substrate. A central composite face-centered design algorithm implemented in MODDE 9.0 was used to generate an experimental setup, consisting of nine experiments plus three replicated center points (Table 3). The results of 11 runs were fitted with multiple linear regression (MLR) producing a quadratic model of excellent statistical quality (see the Supporting Information).

The contour plot illustrates how 1-fluorooctane selectivity and yield change in response to the changes in temperature and solvent polarity (Figure 2). Both responses are nonlinear. The yield of 1-fluorooctane benefits from high temperatures and polar solvent, whereas the corresponding selectivity is higher at the lower values of these parameters.

A so-called "sweet spot" graph shows the optimal operating region, which is located approximately in the center of the graph and corresponds to the median values of temperature and solvent polarity (Figure 3). A simplex-driven software optimizer included with MODDE predicted the highest yield and selectivity at 120 °C and 46:54 tmeu/Mes.

Fluorination: the substrate scope: The optimized reaction conditions were used to investi-

Table 3. Optimization: central composite face-centered design and results for fluorination of 1-chlorooctane with P_2^{Et}·HF.[a]

Entry	Temp. [°C]	tmeu [vol %][b]	Yield [%][c]	Selectivity [%][d]
1	100	0	3	66
2	150	0	19	58
3	100	100	22	58
4	150	100	34	49
5	100	50	18	75
6	150	50	36	60
7	125	0	16	67
8	125	100	31	51
9	125	50	33	74
10	125	50	33	75
11	125	50	29	69

[a] Reaction conditions: 1-chlorooctane, P_2^{Et}·HF (0.18 M), 1 h. [b] Binary mixture of tetramethylurea (tmeu) and mesitylene (Mes). [c] Yield of 1-fluorooctane as determined by GC and/or quantitative NMR spectroscopy. [d] 1-Fluorooctane selectivity is defined as a ratio of 1-fluoroctane to spent 1-chlorooctane, as determined by GC.

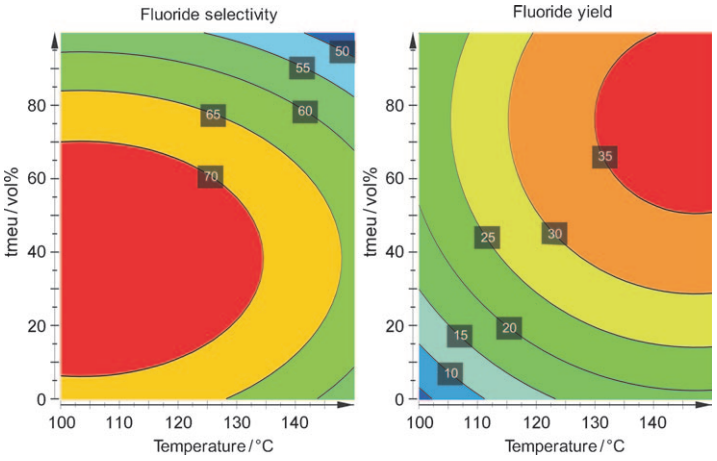

Figure 2. Response surfaces for 1-fluorooctane selectivity and yield as a function of solvent polarity and temperature (see Table 3).

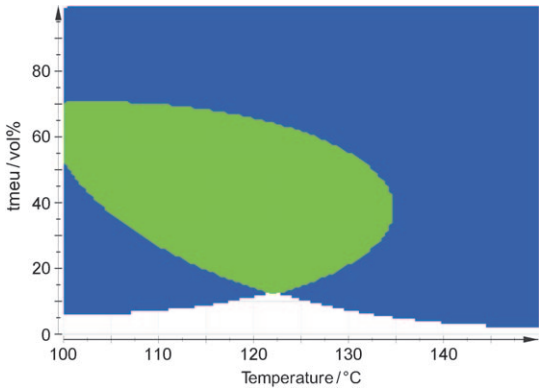

Figure 3. Sweet spot plot as a function of solvent polarity and temperature.

Table 4. Fluorination with P_2^{Et}·HF: the substrate scope.

Entry	Substrate[a]	Yield [%][b]	Alkene [%]	Selectivity [%][c]	Time [min][d]
1	octyl-Cl	72	8	88	180
2	octyl-Br	72	14	78	25
3	octyl-I	59	35	63	10
4	octyl-OMs	76	0	76	<10
5	octyl-OTf	95	0	95	<5
6	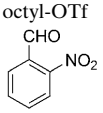	34	–	N/A	320
7	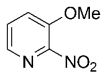	47	–	N/A	180

[a] Substrate (0.18 M), P_2^{Et}·HF (0.28 M, 1.5 equiv) in toluene/DMF or tmeu/Mes (1:1), 120 °C. [b] Yield of the fluorides as determined by GC and/or quantitative NMR spectroscopy. [c] Fluoride selectivity defined as the ratio of fluorinated product to spent substrate. [d] Reactions were run to >90% conversion. Ms: methanesulfonyl, Tf: trifluoromethanesulfonyl, N/A: not applicable.

gate the scope of nucleophilic fluorination and access the relative reactivity and selectivity (Table 4). Alkyl halides were reactive and their reactivity followed the expected order: I > Br > Cl. Unfortunately, the E2 elimination also followed the same order; thus, the selectivity was opposite (Table 4, entries 1–3). Octyl triflate and mesylate reacted within several minutes giving high yields of 1-fluorooctane and no 1-octene. Overall, pseudohalides appear to be the best substrates for fluorination as they react quickly and cleanly.

When reacted with P_2^{Et}·HF, electron-deficient arenes undergo S_NAr fluorination. The nitro group can be substituted to give low-to-moderate yields of aryl fluorides (Table 4, entries 6 and 7).

Table 5 showcases the reactivity of homogeneous P_2^{Et}·HF-based fluorination by comparing it with several other popular nucleophilic fluorination systems. Although biased by the reagent-specific optimization, the results clearly indicate superior reactivity of P_2^{Et}·HF toward 1-chlorooctane.

Radiofluorination: A similar "screen–optimize–run" strategy was adapted for radiofluorination, this time including

Table 5. Comparative performance of different nucleophilic fluorination systems under the same reaction conditions.[a]

Entry	Reagent	Conversion [%]	1-Fluorooctane [%]
1	Et_3N·3HF	5	0
2	proton sponge·HF	1	0
3	KF/Kryptofix 2.2.2	24	4
4	P_2^{Et}·HF	>95	72

[a] Reaction conditions: 1-chlorooctane (1 equiv, 0.18 M), fluorination reagent 1.5 equiv/F in tmeu/Mes (1:1), 120 °C, 3 h.

reaction temperature as an additional reaction factor. Our software-generated screening reaction matrix now contained solvent, temperature, reaction vessel material, and H_2O as the reaction factors, and radiochemical yield as a single response. Table 6 lists the results of the 20 experiments that used 1-naphthalenethyl methanesulfonate as a substrate and the putative P_2^{Et}·[^{18}F]HF as radiofluorination reagent.

Despite good reproducibility (Table 6, entries 9–11), no statistically valid model emerged from radiofluorination screening (see the Supporting Information). Visual inspection of Table 6 also revealed no discernable pattern. Although the insensitivity of radiofluorination to H_2O and reaction vessel material was not surprising given the results of fluorination screening, a solvent and temperature dependence was anticipated. Although at this stage of development the rationalization of these observations is largely speculative, we recognized that a "no model" outcome does not rigorously rule out the importance of the screened factors. Rather, it may indicate that these are masked by some dominant factor(s), which we have not yet been able to identify, for example the presence of impurities acting as an [^{18}F]fluoride trap. Further experiments showed that the ex-

Table 6. Radiofluorination screening: fractional factorial resolution IV design and results for radiofluorination of 1-naphthalenethyl methanesulfonate with P_2^{Et}·[^{18}F]HF.[a]

Entry	Solvent	Temp. [°C]	Reaction vessel	H_2O [μL]	Time [min]	RCY [%][b]
1	toluene	80	copper	10	45	0
2	DMF	80	copper	0	15	60±9
3	toluene	140	copper	0	45	39±7
4	DMF	140	copper	10	15	60±7
5	toluene	80	glass	10	15	42±6
6	DMF	80	glass	0	45	59±4
7	toluene	140	glass	0	15	86±5
8	DMF	140	glass	10	45	84±8
9	toluene	110	copper	5	30	42±6
10	toluene	110	copper	5	30	43±7
11	toluene	110	copper	5	30	45±8
12	toluene	80	copper	0	15	83±9
13	DMF	80	copper	10	45	29±3
14	toluene	140	copper	10	15	88±7
15	DMF	140	copper	0	45	57±5
16	toluene	80	glass	0	45	91±4
17	DMF	80	glass	10	15	28±2
18	toluene	140	glass	10	45	81±9
19	DMF	140	glass	0	15	83±4
20	toluene	110	copper	5	30	58±7

[a] Reaction conditions: 1-naphthalenethyl methanesulfonate (10 mg), solvent (2 mL). [b] Radiochemical yield, determined as an average of two runs.

perimental conditions, optimized for fluorination, are also suitable for radiofluorination. We also found that a tmeu/Mes mixture could be substituted for toluene without any noticeable loss in radiochemical yield. Consequently, the substrate scope was examined at 120 °C in toluene (Table 7). In parallel with fluorination, alkyl pseudohalides proved to be excellent substrates, consistently giving high radiochemical yields (Table 7, entries 2–4). Importantly, mannose triflate can be converted into [^{18}F]fluorodeoxyglucose ([^{18}F]FDG) without any loss of stereochemical integrity (Table 7, entry 1). We were pleased to find that our new radiofluorination protocol was fully compatible with highly lipophilic substrates, such as the mesylate of glycerol ether (Table 7, entry 2). Although radiofluorination with a conventional [^{18}F]KF/Kryptofix system has repeatedly failed to give more than 5% conversion, the reaction with P_4^{tBu}·[^{18}F]HF in toluene furnished the requested fluoride in 71% yield. In contrast to fluorination, alkyl halides did not perform well in radiofluorination: the highest yield of only 15% was obtained when the leaving group was a bromide (Table 7, entry 6). Nucleophilic substitution of a nitro group in pyridines also proceeded with lower yields. The amount of "cold" [^{19}F]1-(2-fluoroethyl)naphthalene in radiofluorination was below the HPLC detection limit for this substrate

Table 7. Radiofluorination with P_2^{Et}·[^{18}F]HF.

Entry	Substrate[a]	Phosphazene + [^{18}F]HF	RCY [%][b]
1	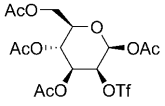	P_4^{tBu}	82 ± 5
2	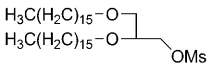	P_4^{tBu}	71 ± 6
3	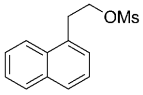	P_2^{Et}	91 ± 4 (81)[c]
4	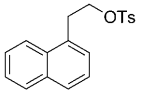	P_2^{Et}	82 ± 6
5	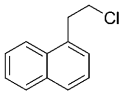	P_2^{Et}	3 ± 1
6	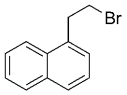	P_2^{Et}	15 ± 2
7	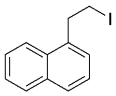	P_2^{Et}	7 ± 2
8	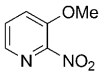	P_2^{Et}	11 ± 3

[a] Substrate (10 mg), P_2^{Et} (10 μL), toluene (2 mL), 120 °C, 30 min. [b] Radiochemical yield, as determined after silica Sep-Pak purification by radio-HPLC and radio-TLC, as an average of three runs. [c] Substrate (1.1 mg), P_2^{Et} (1 μL), toluene (1 mL), 120 °C, 30 min.

(156 ng mL^{-1}), corresponding to specific activity of at least 1.35 Ci μmol^{-1}.

Autofluorolysis of P_1^R·HF: The success of P_2^{Et}·HF and P_4^{tBu}·HF as (radio)fluorination reagents raised the question as to why P_1^{tBu}·HF and P_1^{tOct}·HF gave no (radio)fluorination product. This was even more surprising because the reactivity pattern we described (P_2^{Et}·HF ≈ P_4^{tBu}·HF ⩾ P_1^R·HF) was at odds with the results reported by Lemaire et al.[11] The Belgian group used a number of strong bases including phosphazenes to elute [^{18}F]fluoride from the ion-exchange resin, and performed radiofluorination directly in the eluent. Although the intermediacy of phosphazene hydrofluorides as fluorinating agents was not proven in the report, P_1^{tBu} -containing eluent significantly outperformed its P_2^{Et} analogue. We decided to revisit this issue by examining the reaction between P_1^{tBu}·HF and 1-chlorooctane. Heating the reaction mixture for one hour at 100 °C in [D_8]toluene resulted in the formation of a white precipitate. ^{1}H NMR spectroscopy showed that the solution contained unreacted octyl chloride and no P_1^{tBu}·HF, which suggested that the latter underwent thermal decomposition. This was confirmed by heating a solution of P_1^{tBu}·HF and observing the formation of a precipitate, which was spectroscopically identical to that obtained in the fluorination reaction with 1-chlorooctane. The ^{1}H and ^{13}C NMR spectra of the solid were similar to those of the parent P_1^{tBu}HF, which suggests the presence of $P_1^{tBu}H^+$. However, a peak at $m/z = 144$ (ESI, negative mode), a doublet at −70.4 ppm ($J_{P-F} = 711$ Hz) in the ^{19}F NMR spectrum, and a heptaplet at −143.3 in the ^{31}P NMR spectrum were characteristic of the PF_6^- anion. $P_1^{tBu}H^+PF_6^-$ was previously reported in the literature[20b] and its identity in our reaction was additionally confirmed by its independent synthesis from P_1^{tBu} and HPF_6. It was conceivable that the hexafluorophosphate PF_6^- resulted from the sequence of intra/intermolecular attacks of the fluoride anion on the phosphorus in $P_1^{tBu}H^+$, either via the intermediacy of known alkylamino fluorophosphoranes[31] **B** and **C** or by a direct substitution (Scheme 3).

Regardless of the particularities of the mechanism, a unique susceptibility of P_1^R phosphazene hydrofluorides to fluorolysis was most likely a combination of steric and electronic factors. To investigate the electronics of the system we ran density functional theory (DFT) calculations. Natural bond population analysis performed on $P_1^{tBu}H^+$, $P_2^{Et}H^+$, and $P_4^{tBu}H^+$ optimized at the B3LYP/6-31G* level showed that the positive charge resided mostly on the phosphorus atom and, on average, was the same per phosphorus (2.3–2.4) across the series. The electrophilicity index ω, introduced by Parr[32] and defined as $\omega = \mu^2/2\eta$ (μ is the chemical potential and η is the chemical hardness), was used to rank the phosphazenium cations $P_n^RH^+$ according to their strength as electrophiles.

Table 8 shows that $P_1^{tBu}H^+$ is the strongest electrophile in the series; its electrophilicity index ω is more than four times as high as that of $P_4^{tBu}H^+$ (0.61 vs. 0.14). Among the three phosphazene hydrofluorides $P_1^{tBu}H^+$ has the lowest-

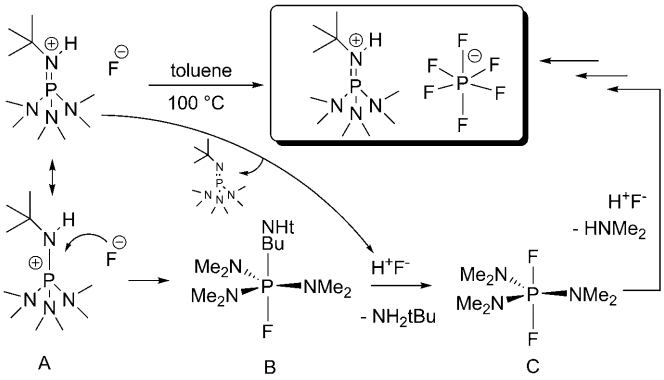

Scheme 3. Possible pathway for autofluorolysis of $P_1^{tBu}HF$ into $P_1^{tBu}HPF_6$.

Table 8. HOMO and LUMO energies and reactivity indices μ, η, and ω for a series of phosphazenium cations calculated at the B3LYP/6-31G* level.

P_n^RHF	HOMO [a.u.]	LUMO [a.u.]	μ [a.u.][a]	η [a.u.][b]	ω [eV]
$P_1^{tBu}H^+$	−0.4028	0.1003	−0.1513	0.5031	0.61
$P_2^{Et}H^+$	−0.3630	0.1233	−0.1198	0.4863	0.40
$P_4^{tBu}H^+$	−0.2945	0.1573	−0.0686	0.4518	0.14

[a] $\mu = (HOMO + LUMO)/2$. [b] $\eta = LUMO - HOMO$.

lying LUMO and the highest hardness η, thus making it the best HSAB (hard and soft acids and bases) match for the hard nucleophile, such as fluoride.[33] Furthermore, the LUMO in $P_1^{tBu}H^+$ is predominantly a P–NMe_2 antibond, which suggests a ready trajectory for nucleophilic substitution of NMe_2 (Figure 4).

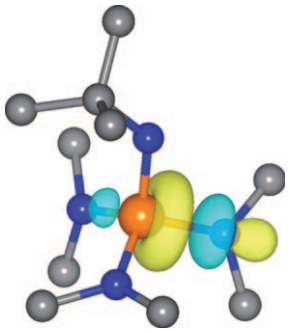

Figure 4. The lowest unoccupied molecular orbital (LUMO) for $P_1^{tBu}H^+$ as calculated at the B3LYP/6-31G* level. Hydrogen atoms are omitted for clarity.

Investigation of space-filled models of the cations indicates that $P_2^RH^+$ and $P_4^RH^+$ are notably bulkier than $P_1^RH^+$, thereby providing increased steric shielding against the nucleophilic attack by the fluoride. The analysis above suggests that the key to stability towards fluorolysis is the increase in steric bulk and electron density on the phosphazenium cation.

Conclusion

We have demonstrated the possibility of a one-step recovery and nucleophilic activation of [^{18}F]fluoride$_{(aq)}$ as [^{18}F]phosphazenium hydrofluorides via the intermediacy of gaseous [^{18}F]HF. With alkyl pseudohalides, phosphazenium [^{18}F]hydrofluorides perform on a par with the conventional [^{18}F]KF/Kryptofix system but significantly outperform the latter if the substrate is lipophilic. The related nonradioactive P_2^{Et}·HF and P_4^{tBu}·HF, easily prepared from the corresponding phosphazene bases and Et_3N·3HF, are efficient reagents for homogeneous fluorination of bromides and pseudohalides. Under DoE optimized conditions, this system is also powerful enough to fluorinate alkyl chlorides in good yields. As revealed by the DoE screening, the system tolerates glass vessels and the presence of water, and can be performed in both polar and nonpolar solvents. In contrast, P_1^{tBu}·HF and P_1^{tOct}·HF are unstable towards autofluorolysis. This can be rationalized in terms of the diminished steric bulk and higher electrophilicity of $P_1^RH^+$. Efforts to automate the radiofluorination process and to minimize [^{18}F]HF recovery time are currently under way.

Experimental Section

General considerations: Unless otherwise noted, all operations were performed under an inert atmosphere of argon. Glassware and reaction vessels were dried in an oven at 160 °C overnight or flame-dried on the Schlenk line prior to use. All fluorination and radiofluorination reactions were performed either in oven-dried screw-cap test tubes made of glass, copper, stainless steel, or glassy carbon, or in flame-sealed NMR tubes. Synthetic procedures for the phosphazenium hydrofluorides were optimized for purity. All solvents and reagents were purchased from Aldrich Co. Unless otherwise noted, diethyl ether, THF, and toluene were distilled from sodium benzophenone; acetonitrile, dichloromethane, DMF, HMPA, tmeu, and Mes were dried over activated molecular sieves (220 °C, 0.1 mbar, 4 h) for at least 48 h prior to use; hexane was used as received. All radiochemical yields were decay-corrected.

Instrumentation: The ultrasound experiments were carried out using a Sonorex DT52H instrument operating at 240 W/35 kHz. ^{1}H, ^{13}C, and ^{31}P NMR spectra were recorded on a Bruker Avance II 500 instrument, at 500, 126, and 202 MHz, respectively. ^{19}F NMR spectra were recorded on a Bruker Avance DPX 250 instrument at 235 MHz. ^{1}H NMR spectra are reported in parts per million (ppm) downfield of TMS and were measured relative to residual protons in deuterated solvents. All ^{13}C NMR spectra are reported in ppm relative to carbon signals in deuterated solvents and were obtained with ^{1}H decoupling. All ^{19}F NMR spectra were obtained without ^{1}H decoupling and were referenced externally relative to C_6F_6. All ^{31}P NMR spectra were ^{1}H decoupled and referenced externally relative to 85 % H_3PO_4. All coupling constants are reported in Hertz. Gas chromatography was performed on a Varian 3900 instrument equipped with a Factor Four capillary column (VF-200ms, 30 m × 0.32 mm I.D., DF = 1.0) and a flame ionization detector. Mass spectrometry was performed on a Bruker Esquire 4000 ion-trap (IT) spectrometer equipped with an electrospray ionization (ESI) interface. Thin-layer chromatography (TLC) was run on precoated plates of silica gel 60 F254 (Merck). ^{18}F aqueous solutions were prepared by an ^{18}O(p,n)^{18}F reaction in a GE PETrace cyclotron with a 1.8 mL target of 95 % enriched [^{18}O]water irradiated by a 14.1 MeV beam at 20–25 mA for 60–90 min. Radio-HPLC was performed by using a Knauer HPLC System K501, equipped with a Knauer RI detector K2301 and CRA radioactivity detector 105 S-1 on a Carbopac PA10 4 × 25 mm Dionex column eluted with

0.1 M NaOH at 1.0 mL min^{-1}. Radio-TLC was performed with a Raytest MiniGita TLC scanner.

Materials and apparatus for [^{18}F]HF production and radiofluorination: The PE, glassy carbon (SIGRADUR) reaction vials, and glass pressure tubes were purchased from Kartell (Italy), HTW Hochtemperatur-Werkstoffe GmbH (Germany), and Aldrich, respectively. The PE tubing (I.D. = 3 mm, O.D. = 4.5 mm) was purchased from Buch & Holm and proved superior to natural rubber Suprene (New Age Industries) in terms of chemical resistance and [^{18}F]fluoride absorption, and was used throughout. The stoppers were made of either PE or Teflon and fitted to the tubing via appropriately sized orifices; no valves were used. All radiochemistry was performed without automation equipment.

Computational methods: The DFT calculations were performed by using the Gaussian 09 suite of programs.[34] All structures were verified to be minima on the potential energy surfaces by vibrational analyses. The optimized structures are given in the Supporting Information as .xyz files. The electron densities were visualized by using VESTA.[35]

General procedure for the synthesis of phosphazene hydrofluorides, P_n^R·HF: A flame-dried 50 mL round-bottomed flask was charged with the corresponding phosphazene base P_n^R (19.69 mmol). The flask was connected to a vacuum line, evacuated, and Et_2O (20 mL) was vacuum-transferred onto the liquid. The flask was then backfilled with Ar, fitted with a rubber septum, and Et_3N·3HF (1.061 g, 6.581 mmol) was added. The reaction mixture was stirred for 1 h, and the product was either filtered under partial vacuum using a double-ended frit or removed by a syringe (P_2^{Et}·HF).

(*tert*-Butylimino)tris(dimethylamino)phosphonium hydrofluoride (P_1^{tBu}·HF): A white solid (54%). ^{1}H NMR (500 MHz, [D$_6$]benzene): δ = 2.47 (d, J = 9.5 Hz, 18H), 1.25 ppm (s, 9H); ^{13}C NMR (126 MHz, [D$_6$]benzene): δ = 32.01 (s, 3C), 37.85 (d, J = 3.6 Hz, 6C), 51.91 ppm (s, 1C); ^{31}P NMR (202 MHz, [D$_6$]benzene): δ = 35.40 ppm (s); ^{19}F NMR (235 MHz, [D$_6$]benzene): δ = −151.18 ppm (br s); MS: m/z: ($P_1^{tBu}H^+$) 235.2 (100%), 236.0 (4%).

(1,1,3,3-Tetramethylbutylimino)tris(dimethylamino)phosphonium hydrofluoride (P_1^{tOct}·HF): A white solid (48%). ^{1}H NMR (500 MHz, [D$_6$]benzene): δ = 1.04 (s, 9H), 1.28 (s, 6H), 1.64 (s, 2H), 2.50 ppm (d, J = 9.8 Hz, 18H); ^{13}C NMR (126 MHz, [D$_6$]benzene): δ = 30.69 (br s, 1C), 31.37 (s, 1C), 31.72 (s, 3C), 37.39 (d, J = 4.5 Hz, 6C), 55.98 (brs, 2C), 56.68 ppm (br s, 1C); ^{31}P NMR (202 MHz, [D$_6$]benzene): δ = 34.87 ppm (s); ^{19}F NMR (235 MHz, [D$_6$]benzene): δ = −152.61 ppm (brs); MS: m/z: ($P_1^{tOct}H^+$) 291.2 (100%), 292.2 (17%).

Tetramethyl[tris(dimethylamino)phosphoranylidene]phosphorictriamid-Et-iminium hydrofluoride (P_2^{Et}·HF): A yellowish viscous oil (77%). ^{1}H NMR (500 MHz, [D$_6$]benzene): δ = 1.43 (td, J = 7.2, 0.6 Hz, 3H), 2.41 (d, J = 10.4 Hz, 18H), 2.59 (d, J = 10.4 Hz, 12H), 2.89–2.98 ppm (m, 2H); ^{13}C NMR (126 MHz, [D$_6$]benzene): δ = 17.95 (d, J = 9.1 Hz, 1C), 36.81 (s, 1C) 37.15 (d, J = 4.5 Hz, 6C), 37.57 (d, J = 4.5 Hz, 4C); ^{31}P NMR (202 MHz, [D$_6$]benzene): δ = 17.66, 18.42 ppm (AB quartet); ^{19}F NMR (235 MHz, [D$_6$]benzene): δ = −150.38 ppm (brs); MS: m/z: ($P_2^{Et}H^+$) 340.3 (100%), 341.2 (18%).

1-*tert*-Butyl-4,4,4-tris(dimethylamino)-2,2-bis-[tris(dimethylamino)phosphoranylidenamino]-2Λ^5,4Λ^5-catenadiphosphazenium hydrofluoride (P_4^{tBu}·HF): A white solid (31%). ^{1}H NMR (500 MHz, [D$_6$]benzene): δ = 1.34 (d, J = 0.6 Hz, 9H), 2.53 ppm (d, J = 10.1 Hz, 54H); ^{13}C NMR (126 MHz, [D$_6$]benzene): δ = 32.27 (d, J = 5.5 Hz, 3C), 37.69 (d, J = 4.5 Hz, 18C), 50.80 ppm (d, J = 3.6 Hz, 1C); ^{31}P NMR (202 MHz, [D$_6$]benzene): δ = −23.63 (q, J = 49.8 Hz, 1P), 12.31 ppm (d, J = 49.8 Hz, 1P); ^{19}F NMR (235 MHz, [D$_6$]benzene): δ = −153.20 ppm (d, J = 119.8 Hz); MS: m/z: ($P_4^{tBu}H^+$) 634.4 (100%), 635.3 (20%), 636.3 (4%).

Fluorination: GC response factor determination: The substrate (0.18 mmol) and naphthalene (internal GC standard, 15 mg) were added to a 1 mL volumetric flask and solvent (tmeu/Mes, 46:54) was added to the mark. A portion (100 μL) of the solution was withdrawn and transferred to a 1 mL volumetric flask. *n*-Hexane was added to the mark and the solution was filtered before injection. The experiment was carried out in triplicate.

Fluorination: general procedure: The substrate (0.18 mmol), P_2^{Et}·HF (1.5 equiv), and naphthalene (15 mg) were added to a 1 mL volumetric flask and the solvent (tmeu/Mes, 46:54) was added to the mark. The reaction mixture was transferred to a glass pressure tube and heated at 120 °C. The initial and final concentrations were determined by GC following the GC response factor determination protocol.

General procedure for [^{18}F]HF generation, transfer, and the synthesis of P_n^R·[^{18}F]HF: [^{18}F]Fluoride (cyclotron target wash, 1 mL, 15–1100 MBq) was added to a reaction vial (PE or glassy carbon) containing H_2SO_4 (98%, 5 mL). The vial was heated for 30 min at 80 °C in an ultrasound bath while being irradiated at 35 kHz. [^{18}F]HF was carried by an argon flow (300–400 scc min^{-1}) to a receiving vial (glassy carbon) containing P_n^R (30 μmol) in toluene or MeCN (2 mL) at 0 °C. The [^{18}F]HF transfer yield was 16–82% measured by the dose calibrator.

Radiosynthesis of 2-[^{18}F]fluoro-2-deoxyglucose ([^{18}F]FDG): The content of the receiving vial (P_2^{Et}·[^{18}F]HF in 2 mL MeCN) was transferred to a glass pressure tube containing mannose triflate (25 mg, 52 μmol) through a stainless steel cannula and the reaction was carried out at 120 °C for 20 min. The reaction mixture was added to a C18 (Waters) cartridge preconditioned with EtOH and H_2O. NaOH (0.70 mL, 2 N) was added to the column and the tetraacetate intermediate was hydrolyzed at room temperature for 5 min. The hydrolyzed product was eluted using H_2O (2 mL). The decay-corrected radiochemical yield was 82%; the radiochemical purity was 98%.

Radiosynthesis of [^{18}F]NpEtF: The content of the receiving vial (P_2^{Et}·[^{18}F]HF in 2 mL toluene) was transferred to a reaction vial (glassy carbon or a glass pressure tube) containing the substrate NpEtOMs (Np: naphthalene, Ms: methanesulfonyl), NpEtOTs (Ts: *p*-toluenesulfonyl), NpEtOTf, NpEtCl, NpEtBr, or NpEtI (52 μmol). [^{18}F] fluorination was carried out at 120 °C for 20 min and [^{18}F] fluorinated product was purified by passing through a Silica Plus (Waters) cartridge. The corresponding radiochemical purities determined by radio-TLC were higher than 99%.

Automated radiochemical synthesis of 3-[^{18}F]fluoro-1,2-di-hexadecylglycerol: [^{18}F]fluoride was recovered from [^{18}O]-enriched water on a QMA SepPak cartridge preconditioned with K_2CO_3. The activity was eluted with 50% acetonitrile in water (0.6 mL) containing K_2CO_3 (7.0 mg, 50.8 μmol) and Kryptofix 2.2.2 (22.0 mg, 58.5 μmol). The eluate was transferred to a ROTEM reactor vial and the acetonitrile/water solution was evaporated under reduced pressure (60 mbar) by using a series of temperature jumps and a helium stream (100 followed by 200 mL min^{-1}). Residual water was removed by azeotropic evaporation with acetonitrile (3 × 0.3 mL). MsO-1,2-di-hexadecylglycerol (5 mg, 8.0 μmol) was added in toluene (0.5 mL) and the solvent was evaporated. Dry DMSO (1 mL) was added and the mixture was allowed to react for 20 min at 165 °C. The reaction mixture was analyzed by radio-TLC, which showed the target compound was obtained with a radiochemical conversion of 2.8%.

Acknowledgements

This research was supported by the Hevesy Laboratory. We thank Palle Rasmussen and Michael Jensen for discussions.

[1] S. M. Ametamey, M. Honer, P. A. Schubiger, *Chem. Rev.* **2008**, *108*, 1501–1516.
[2] S. Purser, P. R. Moore, S. Swallow, V. Gouverneur, *Chem. Soc. Rev.* **2008**, *37*, 320–330.
[3] O. Jacobson, X. Chen, *Curr. Top. Med. Chem.* **2010**, *10*, 1048–1059.
[4] J. Talbot, Y. Petegnief, K. Kerrou, F. Montravers, D. Grahek, N. Younsi, *Nucl. Instrum. Methods Phys. Res. Sect. A* **2003**, *504*, 129–138.
[5] a) L. Cai, S. Lu, V. W. Pike, *Eur. J. Org. Chem.* **2008**, 2843–2843; b) H. H. Coenen, P. H. Elsinga, R. Iwata, M. R. Kilbourn, M. R. A. Pillai, M. G. R. Rajan, H. N. Wagner, J. J. Zaknun, *Nucl. Med. Biol.* **2010**, *37*, 727–740.
[6] R. Krasikova, *PET Chem.* **2007**, *64*, 289–316.

[7] C.-C. Lee, G. Sui, A. Elizarov, C. J. Shu, Y.-S. Shin, A. N. Dooley, J. Huang, A. Daridon, P. Wyatt, D. Stout, H. C. Kolb, O. N. Witte, N. Satyamurthy, J. R. Heath, M. E. Phelps, S. R. Quake, H.-R. Tseng, *Science* **2005**, *310*, 1793–1796.
[8] C.-G. Zhan, D. a. Dixon, *J. Phys. Chem. A* **2004**, *108*, 2020–2029.
[9] a) D. W. Kim, H.-j. Jeong, S. T. Lim, *Nucl. Med. Mol. Imaging* **2010**, *44*, 25–32; b) D. W. Kim, D.-S. Ahn, Y.-H. Oh, S. Lee, H. S. Kil, S. J. Oh, S. J. Lee, J. S. Kim, J. S. Ryu, D. H. Moon, D. Y. Chi, *J. Am. Chem. Soc.* **2006**, *128*, 16394–16397.
[10] D. W. Kim, Y. S. Choe, D. Y. Chi, *Nucl. Med. Biol.* **2003**, *30*, 345–350.
[11] C. F. Lemaire, J. J. Aerts, S. Voccia, L. C. Libert, F. Mercier, D. Goblet, A. R. Plenevaux, A. J. Luxen, *Angew. Chem.* **2010**, *122*, 3229–3232; *Angew. Chem. Int. Ed.* **2010**, *49*, 3161–3164.
[12] J. Aerts, S. Voccia, C. Lemaire, F. Giacomelli, D. Goblet, D. Thonon, A. Plenevaux, G. Warnock, A. Luxen, *Tetrahedron Lett.* **2010**, *51*, 64–66.
[13] S. A. Toorongian, G. K. Mulholland, D. M. Jewett, M. A. Bachelor, M. R. Kilbourn, *Int. J. Radiat. Appl. Instrum., B. Nucl. Med. Biol.* **1990**, 17, 273–279.
[14] J. Simons, *Chem. Rev.* **1931**, *8*, 213–235.
[15] G. A. Olah, J. T. Welch, Y. D. Vankar, M. Nojima, I. Kerekes, J. A. Olah, *J. Org. Chem.* **1979**, *44*, 3872–3881.
[16] a) R. Franz, *J. Fluorine Chem.* **1980**, *15*, 423–434; b) J. M. Kremsner, M. Rack, C. Pilger, O. C. Kappe, *Tetrahedron Lett.* **2009**, *50*, 3665–3668; c) M. A. McClinton, *Aldrichimica Acta* **1995**, *28*, 31–35.
[17] a) I. Bucsi, B. Török, A. I. Marco, G. Rasul, G. K. S. Prakash, G. a. Olah, *J. Am. Chem. Soc.* **2002**, *124*, 7728–7736; b) N. Yoneda, *Tetrahedron* **1991**, *47*, 5329–5365.
[18] a) R. D. Chambers, S. R. Korn, G. Sandford, *J. Fluorine Chem.* **1994**, *69*, 103–108; b) R. D. Chambers, T. F. Holmes, S. R. Korn, G. Sandford, *J. Chem. Soc. Chem. Commun.* **1993**, 855–856; c) M. Darabantu, T. Lequeux, J.-C. Pommelet, N. Plé, A. Turck, L. Toupet, *Tetrahedron Lett.* **2000**, *41*, 6763–6767.
[19] G. Pascali, D. O. Kiesewetter, P. A. Salvadori, W. C. Eckelman, *J. Label. Compd. Radiopharm.* **2004**, *47*, 373–383.
[20] a) R. Schwesinger, R. Link, P. Wenzl, S. Kossek, M. Keller, *Chem. Eur. J.* **2006**, *12*, 429–437; b) R. Schwesinger, J. Willaredt, H. Schlemper, M. Keller, D. Schmitt, H. Fritz, *Chem. Ber.* **1994**, *127*, 2435–2454.
[21] R. Schwesinger, R. Link, P. Wenzl, S. Kossek, *Chem. Eur. J.* **2006**, *12*, 438–445.
[22] S. Re, *J. Phys. Chem. A* **2001**, *105*, 9725–9735.
[23] D. W. Kim, H.-J. Jeong, S. T. Lim, M.-H. Sohn, J. a. Katzenellenbogen, D. Y. Chi, *J. Org. Chem.* **2008**, *73*, 957–962.
[24] J. H. Clark, *Chem. Rev.* **1980**, *80*, 429–452.
[25] D. Landini, A. Maia, A. Rampoldi, *J. Org. Chem.* **1989**, *54*, 328–332.
[26] M. Darabantu, T. Lequeux, J.-C. Pommelet, N. Plé, A. Turck, *Tetrahedron* **2001**, *57*, 739–750.
[27] O. W. Gooding, *Curr. Opin. Chem. Biol.* **2004**, *8*, 297–304.
[28] MODDE 9.0, Umetrics, Umea, http://www.umetrics.com.
[29] C. Reichardt, *Solvent Effects in Organic Chemistry*, Verlag Chemie, Weinheim, **1979**.
[30] a) K. Omura, D. Swern, *Tetrahedron* **1978**, *34*, 1651–1660; b) T. Giagou, M. P. Meyer, *J. Org. Chem.* **2010**, *75*, 8088–8099.
[31] M. Kopp, B. Neumüller, *Z. Anorg. Allg. Chem.* **1999**, *625*, 363–367.
[32] R. Parr, L. Szentpály, S. Liu, *J. Am. Chem. Soc.* **1999**, *121*, 1922–1924.
[33] R. G. Pearson, J. Songstad, *J. Am. Chem. Soc.* **1967**, *89*, 1827–1836.
[34] Gaussian 09, Revision A.02, M. J. Frisch, G. W. Trucks, H. B. Schlegel, G. E. Scuseria, M. A. Robb, J. R. Cheeseman, G. Scalmani, V. Barone, B. Mennucci, G. A. Petersson, H. Nakatsuji, M. Caricato, X. Li, H. P. Hratchian, A. F. Izmaylov, J. Bloino, G. Zheng, J. L. Sonnenberg, M. Hada, M. Ehara, K. Toyota, R. Fukuda, J. Hasegawa, M. Ishida, T. Nakajima, Y. Honda, O. Kitao, H. Nakai, T. Vreven, J. A. Montgomery, Jr., J. E. Peralta, F. Ogliaro, M. Bearpark, J. J. Heyd, E. Brothers, K. N. Kudin, V. N. Staroverov, R. Kobayashi, J. Normand, K. Raghavachari, A. Rendell, J. C. Burant, S. S. Iyengar, J. Tomasi, M. Cossi, N. Rega, J. M. Millam, M. Klene, J. E. Knox, J. B. Cross, V. Bakken, C. Adamo, J. Jaramillo, R. Gomperts, R. E. Stratmann, O. Yazyev, A. J. Austin, R. Cammi, C. Pomelli, J. W. Ochterski, R. L. Martin, K. Morokuma, V. G. Zakrzewski, G. A. Voth, P. Salvador, J. J. Dannenberg, S. Dapprich, A. D. Daniels, Ö. Farkas, J. B. Foresman, J. V. Ortiz, J. Cioslowski, D. J. Fox, Gaussian, Inc., Wallingford CT, **2009**.
[35] K. Momma, F. Izumi, *J. Appl. Crystallogr.* **2008**, *41*, 653–658.

Received: February 10, 2011
Revised: April 5, 2011
Published online: May 30, 2011

